Ultrafast Brain Imaging with Deep-Learning Multi-Shot EPI: Technical Implementation

Bryan Clifford[1], John Conklin[2], Susie Y. Huang[2], Thorsten Feiweier[3], Zahra Hosseini[4], Azadeh Tabari[2], Augusto Lio M. Goncalves Filho[2], Serdest Demir[2], Wei-Ching Lo[1], Stephan Kannengiesser[3], Dominik Nickel[3], Min Lang[2], Maria Gabriela Figueiro Longo[2], Michael Lev[2], Pam Schaefer[2], Otto Rapalino[2], Kawin Setsompop[5], Berkin Bilgic[6], Stephen Cauley[6]

[1]Siemens Medical Solutions USA, Boston, MA, USA
[2]Department of Radiology, Massachusetts General Hospital, Boston, MA, USA
[3]Siemens Healthineers, Erlangen, Germany
[4]Siemens Medical Solutions USA, Atlanta, GA, USA
[5]Department of Radiology and Department of Electrical Engineering, Stanford University, Stanford, CA, USA
[6]Department of Radiology, A. A. Martinos Center for Biomedical Imaging, Massachusetts General Hospital, Harvard Medical School, Boston, MA, USA

This work was performed using a prototype that led to the development of the Deep Resolve Swift Brain product.

Introduction

MRI is a crucial tool for the diagnosis and treatment planning of neurological diseases. Compared to CT and ultrasound, however, the underlying physics of the MR imaging process necessitates relatively long acquisition times. This has limited the use of brain MRI in time- or motion-sensitive settings, such as the emergency department, where long or repeated scans can delay urgently needed treatment [1–4].

The integration of parallel imaging (PI) and simultaneous multi-slice (SMS) imaging techniques [5–8] into standard turbo-spin-echo (TSE)-based clinical protocols has allowed for exam times of approximately 10 minutes. Advances in 3D volumetric encoding schemes [9], compressed sensing [10], and deep-learning (DL) reconstruction techniques [11–13] have helped alleviate the geometry-factor (*g*-factor) noise amplification of standard PI and SMS techniques to provide additional acceleration and further reduce exam times. Current application of these techniques to standard TSE-based protocols has lead to exam times of approximately 5 minutes [14–16].

Recently, single-shot echo-planar imaging (ssEPI) has been used to enable ultrafast multi-contrast exams on the order of 1–2 minutes [17, 18]. ssEPI acquisitions acquire all *k*-space lines after a single excitation or "shot" and allow for very rapid scan times, but require longer readout durations and echo times. As such, ssEPI images often suffer from susceptibility-induced geometric distortion as well as signal dropout and pileup artifacts.

To take advantage of the efficiency of EPI while mitigating signal-to-noise (SNR) and susceptibility-induced losses to image quality, we have developed a multi-shot EPI (msEPI)-based prototype[1] that leverages a DL-based image reconstruction to provide high-SNR T1w, T2w, T2*, and T2-FLAIR, complemented by ssEPI diffusion imaging within a 2-minute exam. The prototype's msEPI acquisition acquires readout lines in an interleaved fashion across several shots to achieve shorter echo times and reduce geometric distortion. At the same time, the DL-based image reconstruction produces high-SNR images and limits *g*-factor noise amplification. To provide greater flexibility and robustness to variations in the clinical workflow, the prototype allows each contrast to be acquired individually, in any orientation, and the DL-reconstruction includes a tunable parameter which can be automatically selected to optimize image quality and data fidelity.

In the following sections, we describe the prototype's data acquisition and image reconstruction methods, and provide performance evaluation metrics and preliminary results on clinical data not included during training.

Data acquisition

Prototype sequences were developed for acquiring T1w, T2w, T2*, FLAIR, and diffusion-weighted imaging data. Multi-shot acquisitions with high per-shot undersampling factors were used for all but the DWI sequence, which was

[1]*Work in progress. The application is currently under development and is not for sale in the U.S. and in other countries. Its future availability cannot be ensured.*

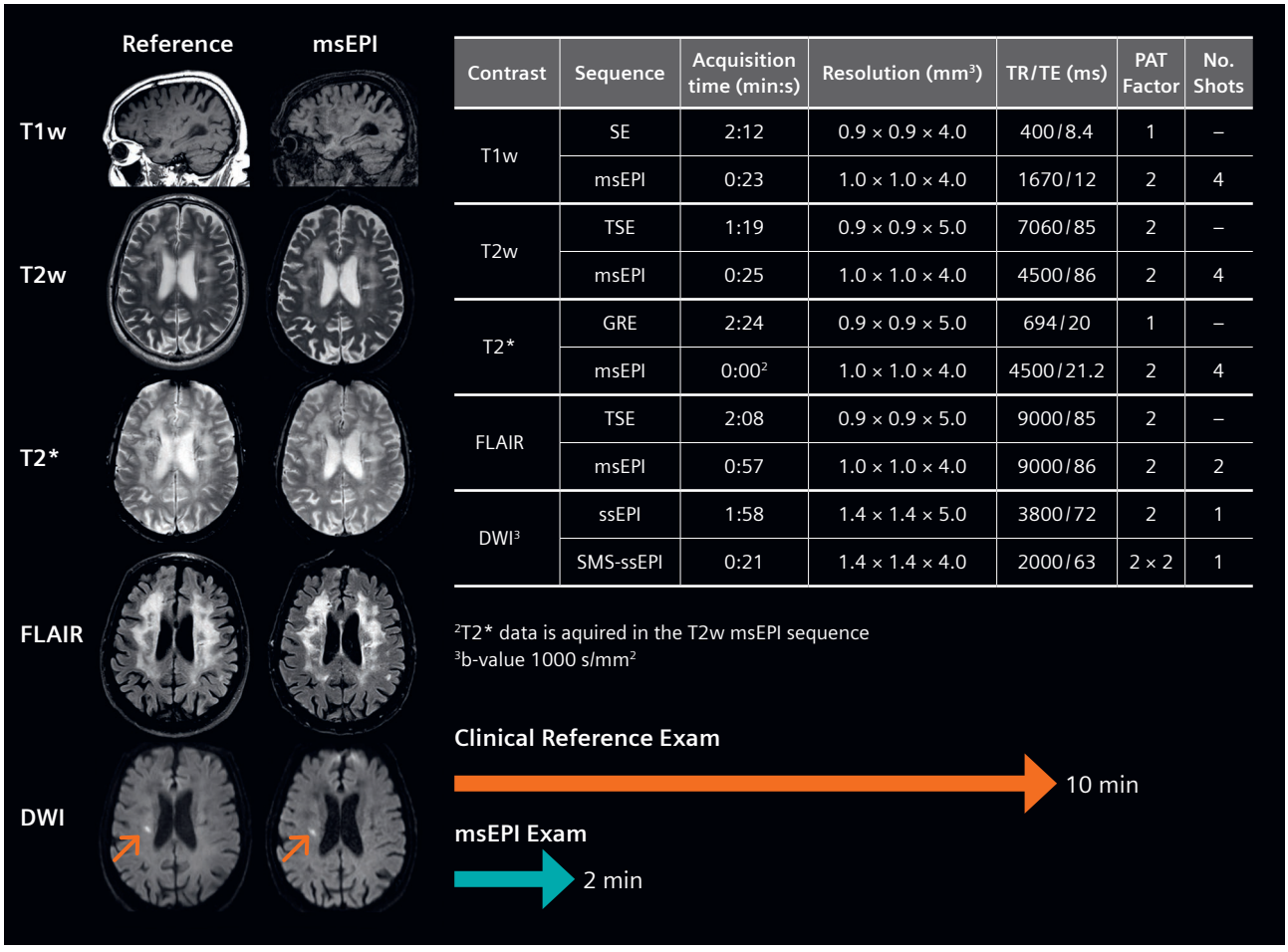
acquired using an SMS ssEPI acquisition. T2w and T2* contrasts are obtained before and after the refocusing pulse of the same msEPI scan, which further increases the sampling efficiency. To provide robustness against intra-scan motion and allow for the individual acquisition of any contrast, each scan was preceded by a fast FLASH reference scan [19], which was used to compute coil sensitivity maps, GRAPPA [5], and/or SMS kernels [20]. Additional information on the data acquisition is provided in [21].

Clinical evaluation data were acquired on patients and healthy volunteers using a 20-channel head/neck coil and a 64-channel head coil on 3T systems (MAGNETOM Prisma and Vida, Siemens Healthcare, Erlangen, Germany) with informed written consent and in accordance with local IRB guidelines. Clinical reference data were acquired for comparison immediately before the prototype exam using a standard 10-minute clinical exam. Protocol parameters from both exams are shown in Figure 1.

A deep-learning network was trained using a dataset consisting of more than 26,000 images across T1w, T2w, T2*, and T2-FLAIR contrasts in axial, coronal, and sagittal orientations (Fig. 2). The 2-average data for network training and validation were acquired on a 3T system (MAGNETOM Skyra, Siemens Healthcare, Erlangen, Germany) using a 20-channel head/neck coil.

Deep-learning hybrid image reconstruction

The prototype sequences use a novel image reconstruction algorithm that integrates DL priors into an iterative SENSE [22] reconstruction (Fig. 3). Undersampled data acquired from the scanner are first passed through a standard



Contrast	Sequence	Acquisition time (min:s)	Resolution (mm³)	TR/TE (ms)	PAT Factor	No. Shots
T1w	SE	2:12	0.9 × 0.9 × 4.0	400/8.4	1	–
	msEPI	0:23	1.0 × 1.0 × 4.0	1670/12	2	4
T2w	TSE	1:19	0.9 × 0.9 × 5.0	7060/85	2	–
	msEPI	0:25	1.0 × 1.0 × 4.0	4500/86	2	4
T2*	GRE	2:24	0.9 × 0.9 × 5.0	694/20	1	–
	msEPI	0:00[2]	1.0 × 1.0 × 4.0	4500/21.2	2	4
FLAIR	TSE	2:08	0.9 × 0.9 × 5.0	9000/85	2	–
	msEPI	0:57	1.0 × 1.0 × 4.0	9000/86	2	2
DWI[3]	ssEPI	1:58	1.4 × 1.4 × 5.0	3800/72	2	1
	SMS-ssEPI	0:21	1.4 × 1.4 × 4.0	2000/63	2 × 2	1

[2]T2* data is aquired in the T2w msEPI sequence
[3]b-value 1000 s/mm²

1 Preliminary clinical results and protocol parameters of the msEPI and clinical reference exam. Images were obtained from a patient not included in the training or validation datasets, with a recent right corona radiata lacunar infarct (DWI images, arrows) and extensive white matter T2-FLAIR hyperintense signal abnormality likely related to cerebral small vessel disease. A graphical representation of the total acquisition times in the clinical reference and msEPI exams is included below the parameter table.

parallel imaging reconstruction, e.g., SENSE, which is used as input to an unrolled gradient-descent network (UGDN) [11]. The UGDN removes residual aliasing artifacts and noise from the initial reconstruction by iteratively passing the image through a deep neural network followed by a data-fidelity increasing operation which incorporates the physics of the acquisition and original measured data. The output of the UGDN, which will have good SNR but may be overly smooth, is then refined in a second iterative SENSE reconstruction, referred to as the DL-SENSE hybrid reconstruction [21].

The DL-SENSE hybrid reconstruction uses the image from the UGDN to regularize an iterative SENSE reconstruction and so generate a high-SNR image with good data fidelity and preservation of fine details. Specifically, the DL-SENSE hybrid reconstruction is a generalization of the methods in [23, 24] and computes the final image by solving the following optimization problem:

$$\min_{\boldsymbol{\rho}} \| \boldsymbol{d} - \Omega \mathrm{FC}\boldsymbol{\rho} \|_2^2 + \lambda \| \mathrm{WFC}(\boldsymbol{\rho}_{\mathrm{UGDN}} - \boldsymbol{\rho}) \|_2^2$$

where $\boldsymbol{d}$ and $\boldsymbol{\rho}$ are vectors of the measured data and image values, respectively; $\boldsymbol{\rho}_{\mathrm{UGDN}}$ is the output of the UGDN; F and C are the Fourier encoding and coil sensitivity operators; Ω is the *k*-space sampling operator; λ is a tunable denoising parameter; W is a diagonal weighting matrix.

A key feature of the DL-SENSE hybrid reconstruction is its ability to provide explicit control over the way the UGDN influences the final reconstructed image, which allows the same network to be applied to data acquired under novel noise conditions without the need for costly retraining. The user can control the balance between the fidelity of the final image with the measured data (left term in the above optimization problem) and with the output of the UGDN (right term in the above optimization problem) by tuning the denoising parameter λ. Similarly, the weighting matrix W controls the spectral mixing of information from the UGDN image and the measured data. In the current prototype, W was chosen as a sampling operator with the same undersampling factor as Ω but with complementary sample locations. For a given value of λ, this choice of W provided a desirable tradeoff between data fidelity and image quality and helped to focus the UGDN's representational power on unsampled *k*-space regions during training.

Network training and validation

The UGDNs used by the prototype were trained using images from a dataset consisting of more than 26,000 images across all contrasts and orientations (Fig. 2). During training, simulated training examples were generated by retrospectively undersampling high-SNR images, and noise was added to the simulated data to match clinical SNR levels. Separate UGDNs were trained for undersampling (PAT) factors of 2, 3, and 4. Networks were trained to minimize a loss function consisting of a weighted combination of the structural similarity index measure (SSIM) – known to correlate with radiologist quality rating [25, 26] – and the mean absolute error between the reconstructed images and their corresponding ground-truths.

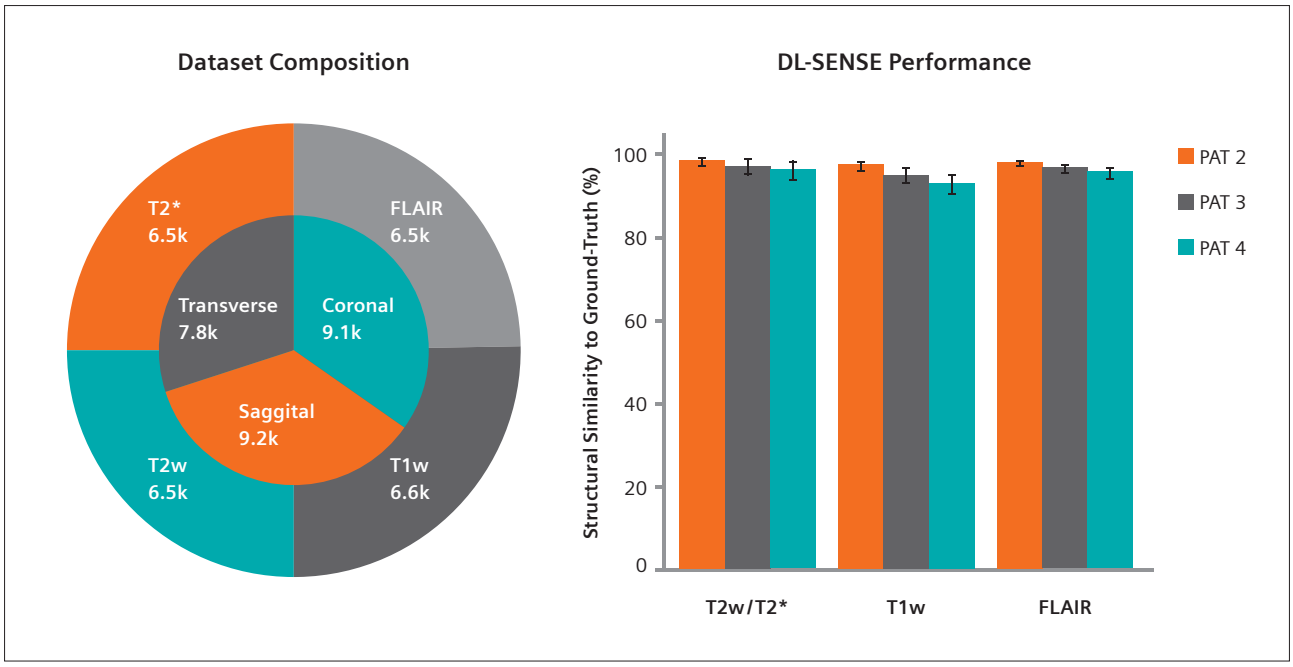
Approximately 6,500 images in the dataset were excluded from training and reserved for validation of the trained networks. Following the same procedure used during training, noisy, undersampled data were generated from these images and reconstructed using the DL-SENSE hybrid scheme. The mean ± SD of the SSIM values between the reconstructed images and their corresponding ground-truth images are shown in Figure 2, sorted by contrast and PAT factor. These results indicate that the proposed method can reliably generate high-quality images, even at higher (≥ 3) acceleration factors.

Automatic selection of the denoising parameter

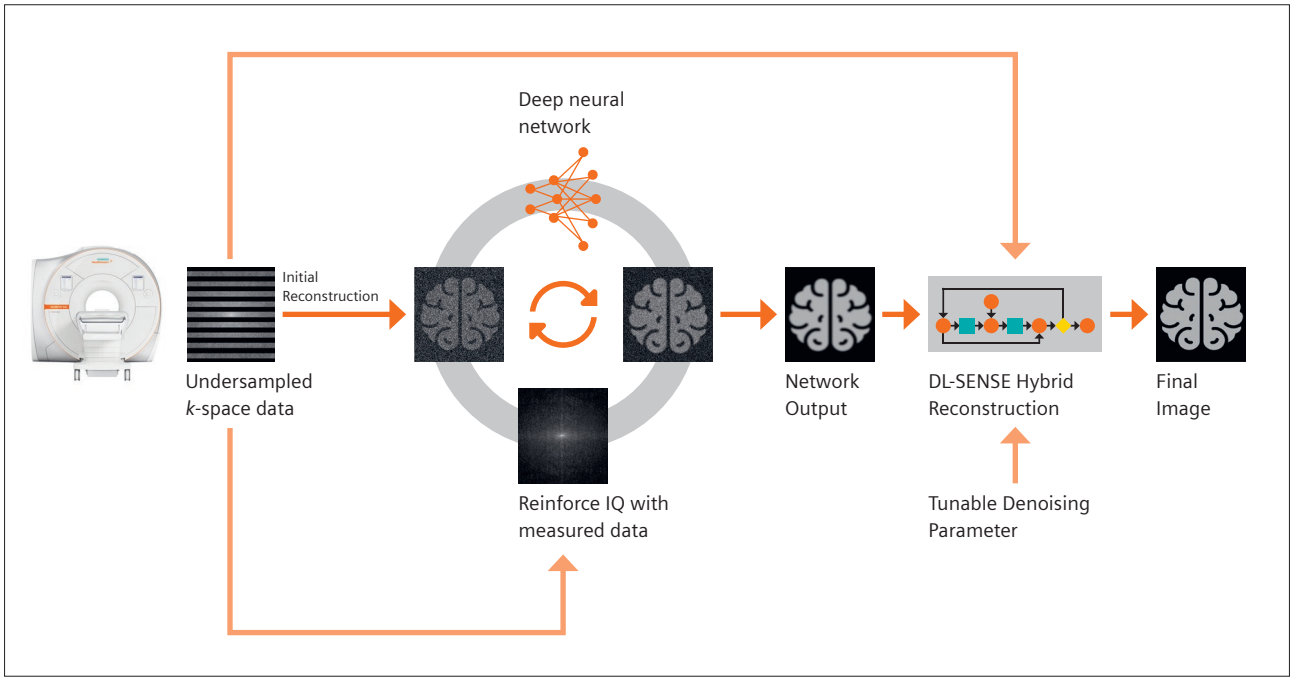
It can be challenging to select an appropriate denoising parameter given the variability seen in clinical settings. For a given protocol, the denoising parameter can be manually tuned according to radiologist preference; however, the ideal choice can vary with changes to protocol parameters, coil loading, coil selection, etc., which are common in the clinic. The parameter that yields the best results in one scenario may lead to overly smooth or noisy images in another scenario.

This problem was addressed by training a model to automatically select the denoising parameter based on estimated data SNR. The prototype computes the noise level using acquisition-specific noise calibration data and combines this with an estimate of the signal intensity to compute the SNR. A trained model then uses the estimated SNR to predict the denoising parameter preferred by radiologists [27]. This automatic, data-driven adaptation of the denoising parameter makes the prototype robust to changes in protocol parameters and automatically reduces the impact of the DL prior on the reconstruction in higher SNR (or lower PAT factor) scenarios, to maximize data fidelity while preserving image quality.

Figure 4A shows both the GRAPPA and DL-SENSE hybrid reconstructions of T2-FLAIR data (the contrast with lowest SNR) acquired from a healthy volunteer at PAT 2, 3, and 4. The GRAPPA reconstructions show the expected noise amplification with increasing PAT factor, but in the DL-SENSE hybrid reconstruction, the noise levels remain



2 Dataset composition and validation results. The dataset consisted of more than 26,000 images and included T1w, T2w, T2*, and T2-FLAIR contrasts as well as coronal, sagittal, and transverse orientations, as shown in the pie chart. The bar chart shows the mean ± SD structural similarity index measure (SSIM) between DL reconstructions and the corresponding ground-truth validation images.



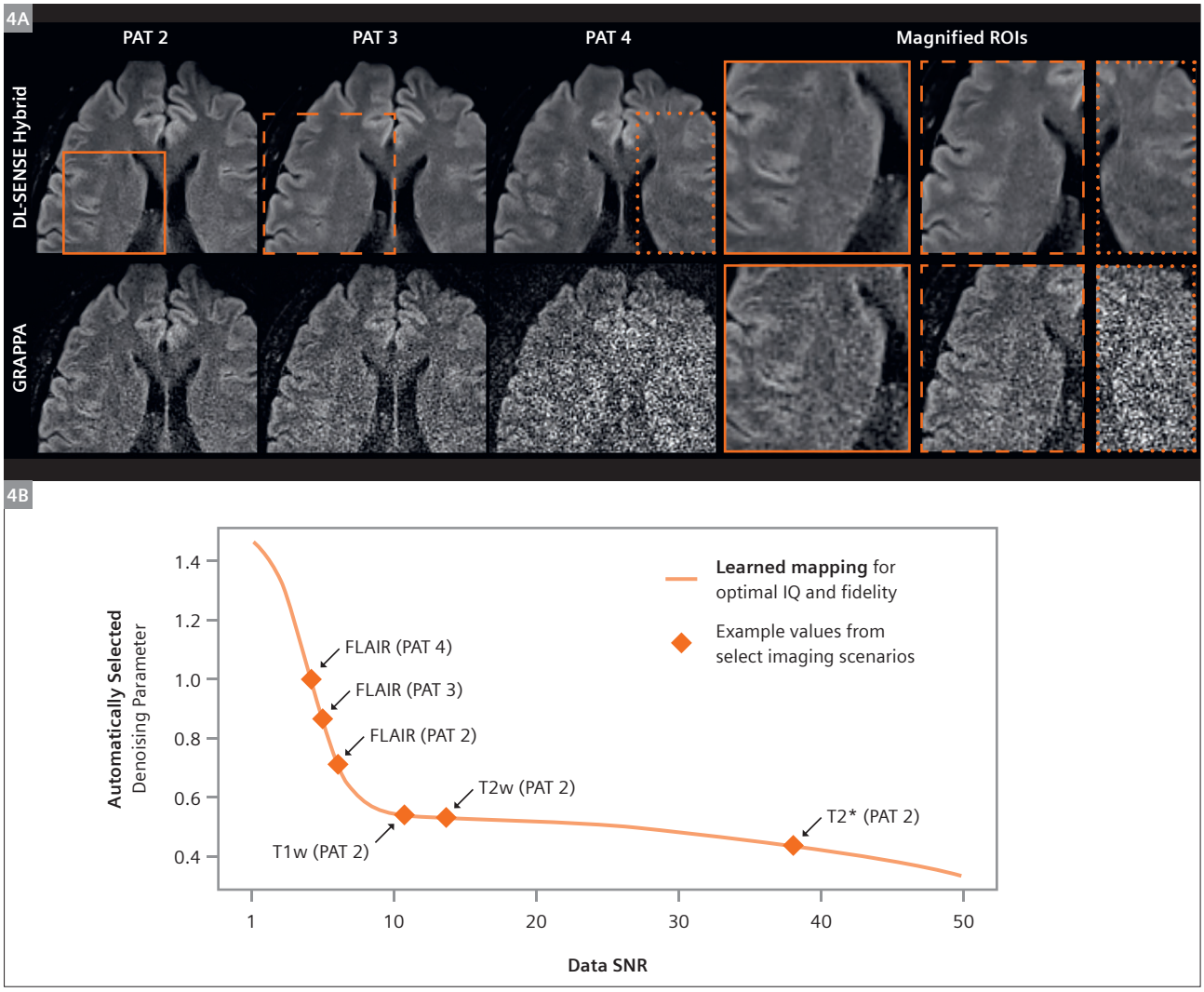
3 Illustration of the proposed reconstruction scheme. An initial SENSE reconstruction is generated from the undersampled *k*-space data and used as input to an unrolled gradient descent network (UGDN). The UGDN repeatedly alternates between deep neural-network denoising and data-fidelity updates to remove noise and residual aliasing while preserving the information in the acquired data. The UGDN output image and the measured data are then used in a regularized DL-SENSE hybrid reconstruction to produce the final image. By incorporating a tunable denoising parameter, the DL-SENSE hybrid reconstruction can be tailored to radiologist preference and also allows the same network to be applied to data acquired under noise conditions not previously seen without retraining.

relatively constant. Examination of representative denoising parameter values (orange markers in Figure 4B) shows that the trained model (orange line in Fig. 4B) automatically adjusts the denoising parameter as the PAT factor increases, using higher values for higher PAT factors. Figure 4B also shows example denoising parameter values from different contrasts and demonstrates how the model uses lower values for higher SNR contrasts (e.g., T2*) as well.

Reconstructions of T2-FLAIR data acquired on the same healthy volunteer using 20- and 64-channel coils are shown in Figure 5. Overall, the SNR of the two images is similar, but in the cortical region, the SNR of the 64-channel image is noticeably higher. These results suggest that the prototype can also adapt to changes in coil selection, allowing users to make the most out of higher density array coils.

Preliminary clinical results

We compared the proposed 2-minute prototype protocol to a standard TSE-based, 10-minute clinical reference protocol on a patient suffering from a recent right corona radiata lacunar infarct (DWI with restricted diffusion, Fig. 1 arrowheads) and extensive patchy and confluent

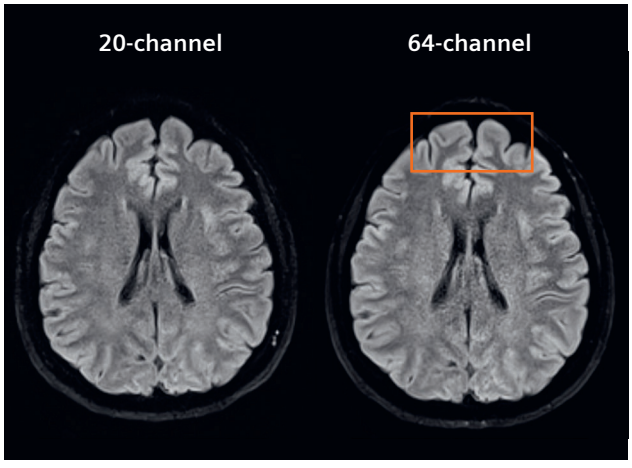


4 Generalization of the DL-SENSE hybrid reconstruction to higher undersampling (PAT) factors and varying SNR levels. **(4A)** Reconstructions of T2-FLAIR data acquired from a healthy volunteer at different PAT factors using the DL-SENSE hybrid reconstruction and GRAPPA. Magnified ROIs displayed on the right show how the proposed DL-SENSE reconstruction automatically adapts the denoising parameter to maintain image quality despite variations in the undersampling factor. **(4B)** The learned mapping between data SNR and optimal denoising parameter (orange line). The mapping was trained to predict parameters chosen by board-certified radiologists. The parameter values for the T2-FLAIR reconstructions in (4A) as well as for representative T1w, T2w, and T2* acquisitions are depicted by orange markers. The trained model tries to provide an optimal balance between image quality and data fidelity; in high-SNR scenarios, the model chooses lower values to maintain image quality while increasing data fidelity.

T2-FLAIR hyperintense white matter signal abnormality likely related to cerebral small vessel disease (T2-FLAIR, Fig. 1). Evaluation of the Figure 1 images by board-certified neuroradiologists indicated that, despite the nearly 5-fold reduction in exam time, the diagnostic quality of the images produced by the prototype was similar to that of the standard 10-minute exam. The white matter signal abnormality as well as the DWI/FLAIR mismatch (indicating a recent infarct) in the infarcted region can be clearly observed in the T2w, T2*, FLAIR, and DWI images from each protocol. Moreover, the gray/white differentiation of the msEPI T1w acquisition is similar to that of the reference SE T1w scan, despite the differences in the respective contrast mechanisms.

Although msEPI T1w images do not optimally depict facial soft tissues, which can be useful in certain diagnostic situations, it is interesting to note that the msEPI T1w images appear to depict the white matter lesions with greater conspicuity than the reference SE acquisition (possibly due to the increased T2* weighting). Regardless, future development will include the evaluation of a GRE-based T1w prototype sequence for the purposes of providing a nearly distortion-free reference, suitable for observing facial soft tissues.

In addition to the results presented here, clinical evaluations of earlier versions of this prototype have also been performed, with similar results [21, 28]. In particular, the report by Tabari et al. [28] provides initial results from a clinical evaluation on a large cohort of inpatients and emergency department patients, which indicate a high degree of interobserver agreement for major diagnostic findings, similar to that of the 5-fold slower clinical reference exam.



5 T2-FLAIR images acquired at 3T with the msEPI prototype sequence using the 20-channel head/neck coil and the 64-channel head coil from Siemens Healthineers. The msEPI prototype automatically adjusts the denoising level according to the SNR in each acquisition scenario, which makes it robust to variations in coil selection. To take advantage of the increased cortical sensitivity of the 64-channel coil, the prototype automatically reduces the denoising parameter in the DL-SENSE hybrid reconstruction to maximize IQ and data fidelity (see highlighted ROI).

Conclusions

We have developed an ultrafast MRI prototype that integrates a highly efficient msEPI acquisition with DL-based image reconstruction techniques to provide comprehensive brain MR imaging in a 2-minute exam. Although clinical evaluation on large patient cohorts is still ongoing, preliminary results indicate that the prototype can automatically adapt its DL reconstruction to variations in protocol parameters and coil selection to produce T1w, T2w, T2*, T2-FLAIR, and diffusion-weighted imaging with diagnostic quality similar to that of a standard 10-minute TSE-based acquisition.

References

1 Agarwal R, Bergey M, Sonnad S, Butowsky H, Bhargavan M, Bleshman MH. Inpatient CT and MRI utilization: trends in the academic hospital setting. J Am Coll Radiol. 2010;7(12):949–955.
2 Selvarajan SK, Levin DC, Parker L. The Increasing Use of Emergency Department Imaging in the United States: Is It Appropriate? AJR Am J Roentgenol. 2019;213(4):W180–W184.
3 Goyal M, Menon BK, van Zwam WH, Dippel DW, Mitchell PJ, Demchuk AM, et al. Endovascular thrombectomy after large-vessel ischaemic stroke: a meta-analysis of individual patient data from five randomised trials. Lancet. 2016;387(10029):1723–1731.
4 Berkhemer OA, Fransen PS, Beumer D, van den Berg LA, Lingsma HF, Yoo AJ, et al. A randomized trial of intraarterial treatment for acute ischemic stroke. N Engl J Med. 2015;372(1):11–20.
5 Griswold MA, Jakob PM, Heidemann RM, Nittka M, Jellus V, Wang J, et al. Generalized autocalibrating partially parallel acquisitions (GRAPPA). Magn Reson Med. 2002;47(6):1202–1210.
6 Pruessmann KP, Weiger M, Scheidegger MB, Boesiger P. SENSE: Sensitivity encoding for fast MRI. Magn Reson Med. 1999;42(5):952–962.
7 Glover GH. Phase-offset multiplanar (POMP) volume imaging: A new technique. J Magn Reson Imaging. 1991;1(4):457–61.
8 Barth M, Breuer F, Koopmans PJ, Norris DG, Poser BA. Simultaneous multislice (SMS) imaging techniques. Magn Reson Med. 2016;75(1):63–81.
9 Bilgic B, Gagoski BA, Cauley SF, Fan AP, Polimeni JR, Grant PE, et al. Wave-CAIPI for highly accelerated 3D imaging. Magn Reson Med. 2015;73(6):2152–2162.
10 Liang D, Liu B, Wang J, Ying L. Accelerating SENSE using compressed sensing. Magn Reson Med. 2009;62(6):1574–84.
11 Hammernik K, Schlemper J, Qin C, Duan J, Summers RM, Rueckert D. Systematic evaluation of iterative deep neural networks for fast parallel MRI reconstruction with sensitivity-weighted coil combination. Magn Reson Med. 2021;86(4):1859–1872.
12 Schlemper J, Caballero J, Hajnal JV, Price AN, Rueckert D. A Deep Cascade of Convolutional Neural Networks for Dynamic MR Image Reconstruction. IEEE Trans Med Imaging. 2018;37(2):491–503.

13 Aggarwal HK, Mani MP, Jacob M. MoDL: Model Based Deep Learning Architecture for Inverse Problems. IEEE Trans Med Imag. 2019;38(2):394–405.
14 Prakkamakul S, Witzel T, Huang S, Boulter D, Borja MJ, Schaefer P, et al. Ultrafast Brain MRI: Clinical Deployment and Comparison to Conventional Brain MRI at 3T. J Neuroimaging. 2016;26(5):503–510.
15 Recht MP, Zbontar J, Sodickson DK, Knoll F, Yakubova N, Sriram A, et al. Using Deep Learning to Accelerate Knee MRI at 3T: Results of an Interchangeability Study. AJR Am J Roentgenol. 2020;215(6):1421–1429.
16 Gassenmaier S, Afat S, Nickel D, Mostapha M, Herrmann J, Othman AE. Deep learning-accelerated T2-weighted imaging of the prostate: Reduction of acquisition time and improvement of image quality. Eur J Radiol. 2021;137:109600.
17 Skare S, Sprenger T, Norbeck O, Rydén H, Blomberg L, Avventi E, et al. A 1-minute full brain MR exam using a multicontrast EPI sequence. Magn Reson Med. 2018;79(6):3045–3054. doi:10.1002/mrm.26974
18 Delgado AF, Kits A, Bystam J, Kaijser M, Skorpil M, Sprenger T, et al. Diagnostic performance of a new multicontrast one-minute full brain exam (EPIMix) in neuroradiology: A prospective study. J Magn Reson Imaging. 2019;50(6):1824–1833.
19 Wang D, Deshpande V, Li X, Urgurbil K. Siemens Healthcare GmbH, Regents of the University of Minnesota, assignee. Multiband Slice Accelerated Imaging With Balanced Slice-Selective Gradients. United States patent 9,989,610. June 5, 2018.
20 Cauley SF, Polimeni JR, Bhat H, Wald LL, Setsompop K. Interslice leakage artifact reduction technique for simultaneous multislice acquisitions. Magn Reson Med. 2014;72(1):93–102.
21 Clifford B, Conklin J, Huang SY, Feiweier T, Hosseini Z, Goncalves Filho ALM, et al. An artificial intelligence-accelerated 2-minute multi-shot echo planar imaging protocol for comprehensive high-quality clinical brain imaging. Magn Reson Med. 2022;87(5):2453–2463. Epub 2021 December 31.
22 Pruessmann KP, Weiger M, Börnert P, Boesiger P. Advances in sensitivity encoding with arbitrary k-space trajectories. Magn Reson Med. 2001;46(4):638–651.
23 Hyun CM, Kim HP, Lee SM, Lee S, Seo JK. Deep learning for undersampled MRI reconstruction. Phys Med Biol. 2018;63(13):135007.
24 Wang S, Su Z, Ying L, Peng X, Zhu S, Liang F, et al. ACCELERATING MAGNETIC RESONANCE IMAGING VIA DEEP LEARNING. In: Proc IEEE Int Symp Biomed Imaging. 2016;2016:514–517.
25 Mason A, Rioux J, Clarke SE, Costa A, Schmidt M, Keough V, et al. Comparison of Objective Image Quality Metrics to Expert Radiologists' Scoring of Diagnostic Quality of MR Images. IEEE Trans Med Imaging. 2020;39(4):1064–1072.
26 Muckley MJ, Riemenschneider B, Radmanesh A, Kim S, Jeong G, Ko J, et al. Results of the 2020 fastMRI Challenge for Machine Learning MR Image Reconstruction. IEEE Trans Med Imaging. 2021;40(9):2306–2317.
27 Hosseini Z, Feiweier T, Conklin J, et al. A data-driven method for automatic regularization selection in a hybrid DL-SENSE reconstruction. In: Proc. Intl. Soc. Magn. Reson. Med. 2022:0206.
28 Tabari A, Clifford B, Goncalves Filho ALM, Hosseini Z, Feiweier T, Lo WC, et al. Ultrafast Brain Imaging with Deep Learning Multi-Shot EPI: Preliminary Clinical Evaluation. ↗ MAGNETOM Flash. 2021;79(2):66–70.

Contact

Bryan Clifford, Ph.D.
Siemens Medical Solutions USA
149 13th St, Suite 2301
Boston, MA 02129
USA
Bryan.Clifford@siemens-healthineers.com

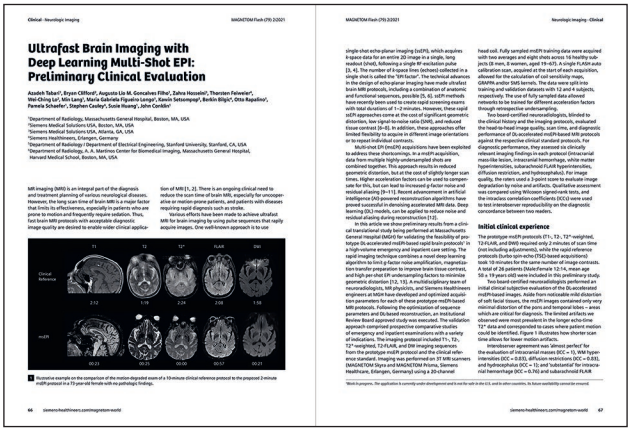


→ Don't miss the clinical aspects of Deep Resolve Swift Brain

John Conklin, Azadeh Tabari, et al. (Massachusetts General Hospital, Boston, MA, USA)

"Ultrafast Brain Imaging with Deep Learning Multi-Shot EPI: Preliminary Clinical Evaluation"

The article is available at
↗ www.magnetomworld.siemens-healthineers.com/clinical-corner/case-studies/deep-resolve-swift-brain



Ultrafast Brain Imaging with Deep Learning Multi-Shot EPI: Preliminary Clinical Evaluation